A Novel Constrained Offset-Free Model Predictive Position Controller for PMSM Drives With a Computationally Efficient Design

Shaobin Li, Mingfei Cai, Liang Zhuo, *Senior Member, IEEE*, Ralph Kennel, *Senior Member, IEEE*, Marcelo Lobo Heldwein, *Senior Member, IEEE*, and Yongxiang Xu

***Abstract*—This article proposes a novel computationally efficient constrained offset-free model predictive position controller (OFMPPC) for surface-mounted permanent magnet synchronous motor (SPMSM). The proposed controller follows a cascaded-free structure based on the system's augmented state space model. Meanwhile, the observability is discussed and a Kalman filter is then incorporated for zero steady state error and robustness improvement. Further, the constraint inequalities are formulated considering all the speed, current and q-axis voltage constraints. And a novel constraint handling strategy is intuitively designed based on the reference governor (RG) theory, where specific modifications are made accordingly to deal with the PMSM application. The detailed design procedure is then given and the constrained OFMPPC with RG is constructed. The proposed method can handle all the constraints but significantly reduce the calculation burden compared with the conventional solver-based quadratic programming solving methods, making model predictive control applicable in real applications. Finally, experiments are conducted based on different scenarios to prove the feasibility and performance of the proposed method.**

***Index Terms*—Offset-free model predictive position controller (OFMPPC), permanent magnet synchronous motor (PMSM), reference governor (RG).**

NOMENCLATURE

η	Smooth factor.
λ	Decision variable of SRG.
ω	Mechanical angular velocity.
ω_c	Cutoff frequency of LPF.
ψ_f	Flux linkage.
τ	Iteration number.
θ	Rotor mechanical position.
d_ω, d_q	Disturbance in speed and q-axis current dynamics.
i_d, i_q	dq-axis current.
L	dq-axis inductance.
N_c	Control horizon.
N_p	Prediction horizon.
p	Number of pole pairs.
R	Stator resistance.
T	Control period.
u_d, u_q	dq-axis voltage.
U_{dc}	DC-link voltage.
v	Output of SRG.
y_m	Measured output.
z	Controlled variable.
z_r	Position reference.
$\omega_{\max}$	Maximum motor speed.
$I_{\max}$	Maximum allowed current.
$I_{q\max}$	Maximum q-axis current.
$U_{q\max}$	Maximum q-axis voltage.

Received 15 January 2025; revised 1 May 2025 and 21 June 2025; accepted 7 August 2025. Date of publication 11 August 2025; date of current version 13 November 2025. Recommended for publication by Associate Editor S.-C. Yang. *(Corresponding author: Yongxiang Xu.)*

Ralph Kennel and Marcelo Lobo Heldwein are with the Chair of High-Power Converter Systems, Technical University of Munich, 80333 Munich, Germany (e-mail: ralph.kennel@tum.de; marcelo.heldwein@tum.de).

Shaobin Li, Mingfei Cai, Liang Zhuo, and Yongxiang Xu are with the School of Electrical Engineering and Automation, Harbin Institute of Technology, Harbin 150001, China (e-mail: flyingshaobin@stu.hit.edu.cn; 22B906063@stu.hit.edu.cn; zhuoliang@hit.edu.cn; xuyx@hit.edu.cn).

Color versions of one or more figures in this article are available at https://doi.org/10.1109/TPEL.2025.3597678.

Digital Object Identifier 10.1109/TPEL.2025.3597678

I. Introduction

PERMANENT magnet synchronous motor (PMSM) has been widely applied to position servosystems due to the inherent features, such as fast control response, high torque density, and high efficiency [1]. And the fast response and high precision requirements for the position servosystems have become increasingly demanding because of the advancement in various high-end applications for example, robotics and aerospace [2], [3].

At present, the most commonly applied PMSM position control scheme is three closed-loop (position, speed and current) PI controller. However, the PI controller cannot guarantee fast response and high precision simultaneously, while the control performance is primarily reduced if parameters or operation conditions change [4]. To solve this, scholars upgrade PI controllers based on the cascaded structure with various advanced techniques. For example, Garcia et al. [5] updated the PI controller with a full predictive cascaded speed and current control to improve the overall control quality. Even if the performance can be improved to some extent, the cascaded structure strongly restricts the dynamics with a limited bandwidth [6], [7], which is undesirable for high-quality position control applications.

In order to increase dynamics, the concept of cascaded-free PMSM position control with model predictive control (MPC) is put forward. This approach fully exploits MPC's advantages,

such as easy constraint handling ability, flexible control objective selection, and friendliness to multivariable high order systems [8], making cascaded-free MPC methods attractive in the PMSM position control field. Among the existing literature, finite-control-set model predictive control (FCS-MPC) belongs to one category of MPC, which minimizes the cost function by a finite number of switching states' combinations [9]. In [10], [11], a cascaded-free predictive position controller based on FCS-MPC is developed considering various control objectives in the cost function. However, its disadvantages include variable switching frequency, complex weighing factor tuning and significant harmonics in response, which handicaps the application of FCS-MPC more or less [12].

In comparison, continuous control set model predictive control (CCS-MPC) utilizes a modulator to achieve a better steady state performance and is usually more appropriate to achieve longer horizon control [13]. For example, He et al. [14] built a position controller by solving the convex optimization problem. Belda and Vosmik [15] dealt with a specific explicit design of generalized predictive control for both speed and position control. However, the biggest challenge lies in constraint handling, and the typical treatment is to use a solver to iteratively solve the quadratic programming (QP) problems. Even if several powerful solvers have been proposed for MPC, for example, active-set based methods [16], gradient projection-based methods [17], nonnegative least square based methods [18], etc., the required computational load of CCS-MPC is typically too high to be applied in microprocessors for real-time online calculation. Hence, the aforementioned CCS-MPC methods can either be applied only for the short horizon case [19] or can hardly be implemented in real applications when a long prediction horizon is selected [20]. Note that a long prediction horizon is necessary for better position control performance since the entire transient dynamics should be covered.

Thanks to the development of control theory, an alternative method to deal with constraints is to employ a reference governor (RG). As its name suggests, the RG technique is an add-on scheme by modifying the reference signal to a well-designed closed-loop system [21]. Typically, RG serves as an intelligent prefilter that modifies the input reference as closely as possible to the given reference command, subject to satisfying all the constraints while preserving the performance of the original closed-loop system [22]. Among all the RG methods, the scalar reference governor (SRG) stands out due to its inherent appeal, presenting computationally straightforward realizations for both linear and nonlinear systems subjected to disturbances and parameter uncertainties [23]. Equipped with SRG, the complex optimization solving process in CCS-MPC can be converted to dealing with a simple 1-D optimization problem and an unconstrained MPC control calculation, which is of great significance [24]. However, RG's potential has not yet been fully exploited in the power electronics and drives field.

Another problem in CCS-MPC is that conventional design hardly guarantees any robustness to disturbances [25]. Hence, if the nominal PMSM model deviates a lot from the real one due to parameter mismatches, unmodeled dynamics or changes in the ambient environment, this deviation will significantly deteriorate the control performance and may even cause system failure [26]. To address this issue, the most applied methods are based on disturbance observer techniques [27], where an external observer, such as the extended state observer [28] and moving horizon estimator [29], is used for estimation and compensation. However, introducing an external loop will compromise the main control performance more or less [26]. A promising solution is to incorporate robustness design into the MPC controller itself, but there is still much to be studied, especially in the PMSM control field.

In this article, a novel constrained offset-free model predictive position controller (OFMPPC) with a computationally efficient design for surface-mounted permanent magnet synchronous motor (SPMSM) is proposed. The main contributions of this article can be concluded by two key points as follows.

1) A novel offset-free MPC position controller is proposed for the first time in the SPMSM control field, overcoming the poor robustness issue in conventional MPC-based methods by incorporating disturbance rejection in the design process. A cascaded-free control structure is adopted to improve the bandwidth, allowing simultaneous control of the q-axis current, motor speed, and position. Meanwhile, a complete design procedure is provided, with a constrained convex optimization problem formulated.
2) A novel constraint handling strategy based on the RG theory is intuitively proposed to solve the constrained optimization problem. In contrast to the conventional solver-based iterative approaches, the proposed OFMPPC-RG method significantly reduces the calculation time, enabling the application of long horizon MPC on real microprocessors. Furthermore, the effectiveness of this innovative method is validated experimentally through a series of comparative studies.

II. System Description and OFMPPC Design

In this section, firstly a full-order SPMSM model considering disturbances is modeled. Based on this, the formulation of the proposed offset-free noncascaded MPC position controller is given, which includes the Kalman filter design and steady state condition calculation.

A. Full-Order-SPMSM Model

For SPMSM, the discrete state space model considering the position control dynamics should be derived. Here, the d-axis current reference i_d^* is always set to zero to achieve the maximum torque per ampere control for PMSM [30]. If the i_d loop controller works well, $i_d = i_d^* = 0$ can be obtained. In such case, the d-axis control can be decoupled from the torque (q-axis) performance [31] and the overall equation can be formulated as (1). This design not only decreases the system's dimension by one for calculation reduction but also improves the transient torque control performance [32]

$$\begin{cases} x(k+1) = Ax(k) + Bu_q(k) + B_d d(k) \\ y_m(k) = Cx(k) \\ z(k) = Hy_m(k) \end{cases} \tag{1}$$

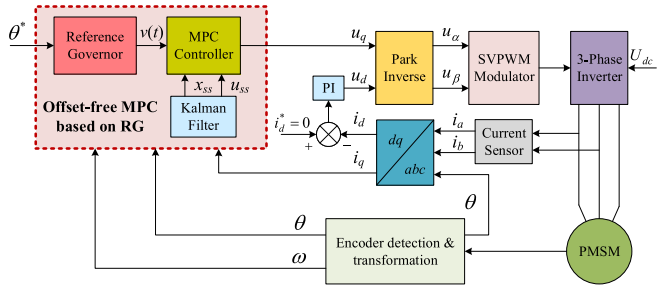

Fig. 1. Block diagram of the proposed OFMPPC for PMSM drives based on RG.

where $A = \begin{bmatrix} 1 & T & 0 \\ 0 & 1 & \frac{3p\psi_f T}{2J} \\ 1 & -\frac{p\psi_f T}{L} & 1-\frac{TR}{L} \end{bmatrix}$; $B = \begin{bmatrix} 0 \\ 0 \\ \frac{T}{L} \end{bmatrix}$

$B_d = \begin{bmatrix} 0 & 0 \\ 1 & 0 \\ 0 & 1 \end{bmatrix}$; $x(k) = \begin{bmatrix} \theta(k) \\ \omega(k) \\ i_q(k) \end{bmatrix}$; $d(k) = \begin{bmatrix} d_\omega(k) \\ d_q(k) \end{bmatrix}$

$y_m(k) = \begin{bmatrix} \theta(k) \\ i_q(k) \end{bmatrix}$; $C = \begin{bmatrix} 1 & 0 & 0 \\ 0 & 0 & 1 \end{bmatrix}$; $H = [1 \quad 0]$; where k is the sampling moment. Also note that in (1), $y_m(k)$ contains position and q-axis current information directly measured by the sensors; $z(k)$ represents the motor position, which should be controlled to track the given reference.

Another point to note about this equation is that the disturbance terms $d_\omega(k)$ and $d_q(k)$ contain the main external and internal disturbances in the q-axis current loop and speed loop, respectively, for example, the modeling error caused by the friction, parameter mismatches, dead time effect, etc. [28]. What is more, the coupling term of i_d in the q-axis loop equation can also be treated as a disturbance when i_d is not controller to be exactly zero in transients. Hence, the position control performance can hardly be affected by this decoupled formulation. Further, the block diagram of the proposed OFMPPC-RG method is shown in Fig. 1, where a well-tuned PI controller is applied for i_d control.

B. Kalman Filter Design

In fact, the accurate observation of the system disturbances $d_\omega(k)$ and $d_q(k)$ is vital for realizing offset-free position tracking. To achieve this, the state space model (1) is augmented as (2) if the dynamics of each element in $d(k)$ is assumed to be slowly varying

$$\begin{cases} x_e(k+1) = A_e x_e(k) + B_e u_q(k) \\ y_m(k) = C_e x_e(k) \end{cases} \tag{2}$$

where the state vector $x_e(k) = [x(k) \quad d(k)]^T$; $B_e = [B \quad 0]^T$; $A_e = \begin{bmatrix} A & B_d \\ 0 & \mathbf{I}_{2\times 2} \end{bmatrix}$; $C_e = [C \quad 0]^T$.

It can be seen that the observability of the augmented system (2) always holds whatever the parameters are. This proof is given in detail in the Appendix section. Therefore, (2) can be further represented with system noise as

$$\begin{cases} x_e(k+1) = A_e x_e(k) + B_e u_q(k) + w(k) \\ y_m(k) = C_e x_e(k) + v(k) \end{cases} \tag{3}$$

where $w = [w_1 \quad \cdots \quad w_5]^T$ and $v = [v_1 \quad v_2]^T$ are the zero mean Gaussian white noise denoting the process noise and measurement noise, respectively, with the covariance

$$E\left\{ \begin{pmatrix} w \\ v \end{pmatrix} \begin{pmatrix} w^T & v^T \end{pmatrix} \right\} = \begin{pmatrix} \mathbf{Q}_0 & 0 \\ 0 & \mathbf{R}_0 \end{pmatrix}.$$

From (3), the Kalman filter for the augmented PMSM system can be designed as (4) according to [33] to estimate all the states and disturbances accurately. Meanwhile, $\mathbf{Q}_0$ and $\mathbf{R}_0$ serve as the tuning matrices

$$\begin{aligned} \hat{x}_e(k+1) = {} & A_e \hat{x}_e(k) + B_e u_q(k) \\ & + \mathbf{L}_f \left(-y_m(k) + C_e \hat{x}_e(k) \right) \end{aligned} \tag{4}$$

where variables with "$\hat{}$" means the estimated states; $\mathbf{L}_f$ is the Kalman filter gain satisfying

$$\mathbf{L}_f = A_e \mathbf{P} C_e^T \left(C_e \mathbf{P} C_e^T + \mathbf{R}_0 \right)^{-1}$$

and the matrix P is the solution of the algebraic Riccati equation [33] with the expression as follows:

$$\mathbf{P} = \mathbf{Q}_0 + A_e \mathbf{P} A_e^T - A_e \mathbf{P} C_e^T \left(C_e \mathbf{P} C_e^T + \mathbf{R}_0 \right)^{-1} C_e \mathbf{P} A_e^T.$$

C. Steady State Condition

To construct the proposed controller, the steady state value should be calculated based on the estimated disturbances. Since the system's disturbance can be regarded as slowly varying, $\hat{d}(\infty) = \hat{d}(k)$ holds for a given PMSM system. Also, $x(k+1) = x(k)$ can be achieved in the steady state. According to (1), the states and the control signal should satisfy (5) if z_r is to be tracked in an offset-free manner

$$\begin{pmatrix} A - \mathbf{I} & B \\ HC & 0 \end{pmatrix} \begin{pmatrix} x_{ss} \\ u_{qss} \end{pmatrix} = \begin{pmatrix} -B_d \hat{d}(\infty) \\ z_r \end{pmatrix} \tag{5}$$

where $x_{ss} = \begin{pmatrix} \theta_{ss} & \omega_{ss} & i_{qss} \end{pmatrix}^T$; θ_{ss}, ω_{ss}, i_{qss}, u_{qss}, and $\hat{d}(\infty)$ denote the corresponding steady state values of each state variable, control signal, and disturbances.

After bringing in all the parameters, (5) has the following unique solution (6):

$$\begin{cases} \theta_{ss} = z_r, i_{qss} = -\frac{2J}{3p\psi_f T} \hat{d}_\omega(k) \\ \omega_{ss} = 0, u_{qss} = -\frac{2JR}{3p\psi_f T} \hat{d}_\omega(k) - \frac{L}{T} \hat{d}_q(k). \end{cases} \tag{6}$$

To conclude, the necessary and sufficient conditions for the offset-free position tracking is that the system's input and output signals precisely converges to the steady state condition in (6), which can be described mathematically as

$$\lim_{k\to\infty} z(k) = z_r, \quad \lim_{k\to\infty} u_q(k) = u_{qss}.$$

D. Offset-Free MPC Controller Design

In this section, the design flow of the proposed predictive position controller is illustrated briefly. Apart from the single loop cascaded-free MPC control idea, the other novelty of our proposed method lies in the offset-free design and the incorporation of the disturbance observer. Following are the detailed steps.

First, assume that ($N_p \geq N_c$), the prediction sequence Z and control sequence U_q can be expressed as follows:

$$Z = \begin{bmatrix} z(k+1|k) & z(k+2|k) & \cdots & z(k+N_p|k) \end{bmatrix}^T$$

$$U_q = \begin{bmatrix} u_q(k|k) & u_q(k+1|k) & \cdots & u_q(k+N_c-1|k) \end{bmatrix}^T.$$

Further, a compact matrix expression of the future outputs can be obtained as (7) according to (1)

$$Z = Fx(k) + \Phi U_q + M\hat{d}(k) \tag{7}$$

where $F = \begin{pmatrix} HCA & HCA^2 & \cdots & HCA^{N_p} \end{pmatrix}^T$

$$M = \begin{pmatrix} HCB_d & HC(AB_d + B_d) & \cdots & HC\sum_{i=0}^{N_p-1} A^i B_d \end{pmatrix}^T$$

$$\Phi = \begin{pmatrix} HCB & 0 & \cdots & 0 \\ HCAB & HCB & \cdots & 0 \\ \vdots & \vdots & & 0 \\ HCA^{N_p-1}B & HCA^{N_p-2}B & \cdots & HCA^{N_p-N_c}B \end{pmatrix}.$$

Due to the relatively long position control transients of the PMSM resulting from large mechanical time constants, a sufficiently long prediction horizon N_p is necessary. This is crucial to encompass the entire transient process, ensuring satisfactory tracking performance, system stability, and robustness [34].

Furthermore, the cost function of the proposed offset-free position controller can be constructed as (8) under the steady-state condition in Section C, where two quadratic terms control the tracking of both the output and input states, respectively. Obviously, the control objective is to navigate all the state variables to track the steady-state final value in the presence of disturbance, so as to cancel the disturbance's effect on the position control and eliminate steady-state errors

$$J_p = (Z_r - Z)^T Q (Z_r - Z) + (U_q - U_{qss})^T W_R (U_q - U_{qss}) \tag{8}$$

where Z_r is an $N_p \times 1$ dimensional vector comprised of the reference positions z_r while U_{qss} is an $N_c \times 1$ dimensional vector containing u_{qss}; $Q = q\mathbf{I}_{N_p \times N_p} (q > 0)$ and $W_R = w_R \mathbf{I}_{N_c \times N_c} (w_R > 0)$ are tunable output and control weighing matrices, respectively, which determine how much emphasis to put on each tracking error.

By substituting (7) into (8), the cost function can be simplified as

$$J_p = \Delta^T Q \Delta + U_{qss}^T W_R U_{qss} + U_q^T (\Phi^T Q \Phi + W_R) U_q - \left(2\Delta^T Q \Phi + 2U_{qss}^T W_R\right) U_q \tag{9}$$

where $\Delta = Z_r - Fx(k) - M\hat{d}(k)$ is used for expression simplicity.

Obviously, the extremum value of (9) in the unconstrained case can be calculated by setting $\partial J_p / \partial U_q = 0$ and the corresponding control sequence can be expressed as

$$U_q = \left(\Phi^T Q \Phi + W_R\right)^{-1} \Phi^T Q \left(Z_r - Fx(k) - M\hat{d}(k)\right) + \left(\Phi^T Q \Phi + W_R\right)^{-1} W_R U_{qss}. \tag{10}$$

Considering about the one and a half control periods' time delay in the digital PMSM control system [26], the second element in the control sequence (10) is taken as the final control signal for delay compensation, which is shown as

$$u_q(k) = E_2 U_q = (\underbrace{0 \quad 1 \quad 0 \quad \cdots \quad 0}_{N_p}) U_q. \tag{11}$$

E. Constraints in the PMSM Position Control

The control derived from (11) cannot be directly applied to a given PMSM position control system. Constraints on both the control voltage and the system states from the so-called "inner loops" (q-axis current and motor speed) should be considered to prevent damage to the drives [19]. In this section, constraint inequalities for the proposed controller are modeled, and the final OFMPPC controller is constructed in the form of a convex QP problem.

1) Current Constraint Inequality: The current constraint is vital to avoid overcurrent in position control drives. In this work, the q-axis current constraint boundary is given considering the d-axis dynamics as

$$-I_{q\,\max} \leq i_q(k+n|k) \leq I_{q\,\max} = \sqrt{I_{\max}^2 - i_d^2(k)} \tag{12}$$

where $n = 1, 2, \ldots, k_q$ is the set of future sampling instants on which to impose constraints.

2) Speed Constraint Inequality: Typically, the motor speed needs to be limited in the case of long-distance tracking to ensure the rotor does not exceed its maximum allowed speed. Hence, the speed constraint inequality should be given as

$$-\omega_{\max} \leq \omega(k+n|k) \leq \omega_{\max} \tag{13}$$

where $n = 1, 2, \ldots, k_\omega$ is the set of future sampling instants to impose constraints on.

Note that speed constraints should be set on more future steps because of the slow speed control dynamics.

3) Voltage Constraint Inequality: Despite speed and current limitations, the output voltage of the controller u_q should also satisfy the maximum output capability of the inverter to prevent overmodulation. Considering this, the boundary of the voltage limitation can be given as

$$-U_{q\,\max} \leq u_q(k+n|k) \leq U_{q\,\max} = \sqrt{U_{\mathrm{dc}}^2/3 - u_d^2(k)}. \tag{14}$$

Therefore, the proposed OFMPPC controller's output can be converted to the solution of a constrained convex QP problem as (15) at every sampling instant k

$$\underset{U_q}{\operatorname{argmin}}\, J_p = (Z_r - Z)^T Q (Z_r - Z) + (U_q - U_{qss})^T W_R (U_q - U_{qss})$$

$$
\begin{aligned}
\text{s.t. } & x\left(k+i+1|k\right)=Ax\left(k+i|k\right)+Bu_q\left(k+i|k\right)+B_d\hat{d}(k)\\
& z\left(k+i|k\right)=HCx\left(k+i|k\right)\\
& x(k|k)=x(k), i=0,1,2,\ldots,N_p\\
& -I_{q\,\max}\le i_q\left(k+n|k\right)\le I_{q\,\max}, n=1,2,\ldots,k_q\\
& -\omega_{\max}\le \omega\left(k+n|k\right)\le \omega_{\max}, n=1,2,\ldots,k_\omega\\
& -U_{q\,\max}\le u_q\left(k+n|k\right)\le U_{q\,\max}, n=1,2.
\end{aligned}
\tag{15}
$$

III. Computationally Efficient Constraint Handling Based on RG

Typically, various optimization methods, such as active-set or interior-point methods [35], are used to solve the constrained QP problem in (15). However, these solvers usually involve a large number of iterations and result in a high computational burden, especially for long horizon MPC problems, which hinders the application of MPC in practical scenarios. To solve this issue, a novel computationally efficient constraint handling method based on SRG theory is discussed in this section.

A. Scalar Reference Governor

Normally, the RG approach deals with a prestabilized closed-loop discrete-time system in the form of

$$
\begin{cases}
x\left(k+1\right)=A_{cl}x(k)+Bv(k)\\
y(k)=Cx(k)+Dv(k)
\end{cases}
\tag{16}
$$

where $x(k)$ is the state vector; $y(k)$ is the output vector; $v(k)$ is the set point of the primary controller. Note that (16) is an asymptotically stable system with the matrix A_{cl} reflecting the closed-loop dynamics and Schur [23] (all eigenvalues strictly reside within the unit circle). Usually, the system is also subject to k_j number convex constraints, which limit both the states and the inputs since $t=k$

$$
c_j\left(x(k),v(k)\right)\le 0,\ \forall j=1,\ldots,k_j.
$$

In short, the idea of a RG is to modify the desired reference $r(k)$ to a prefiltered reference trajectory $v(k)$, which is then given to a well-designed closed-loop system so that the system's constraints will not be violated. The common feature of a RG is that: if $v(k)$ is constantly applied to the system from the time instant $t=k$ onward, all constraints will always get satisfied. The claim mentioned previously can be described by the concept of the maximal constraint admissible set O_∞ in a more formal way as

$$
O_\infty=\left\{(v,x)|c_j\left(x\left(k+\tau\right),v(k)\right)\le 0,\forall\tau\in\mathbb{Z}_+\right\}. \tag{17}
$$

With the concept of O_∞, the formulation of the SRG can be easily illustrated mathematically. Generally, SRG algorithm seeks the optimal point that resides on the line segment between the previous SRG output $v(k-1)$ and the set point value $r(k)$ at each time constant $t=k$ based on the measured state $x(k)$. This point is the closest approximation of $v(k)$ to $r(k)$ and also serves as the reference signal for the closed-loop system (16). More formally, SRG converts the complicated multiobjective optimization problem to a much simpler optimization problem (18)

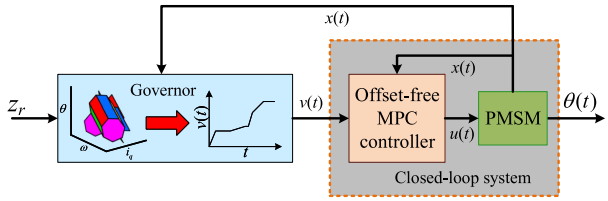

Fig. 2. Hierarchy of the proposed RG and OFMPPC.

with only one decisive variable

$$
\begin{aligned}
&\max\ \lambda\\
&\text{s.t. } \begin{cases}
0\le\lambda\le 1\\
\left(x(k),v(k)\right)\in O_\infty\\
v(k)=\left(1-\lambda\right)v\left(k-1\right)+\lambda r(k)
\end{cases}
\end{aligned}
\tag{18}
$$

where λ is a scalar to be calculated in each sampling period. Obviously, λ is the largest value possible when all the constraints enforce. And in the extreme case, $\lambda=1$ means no constraint violation danger exists even if $r(k)$ is directly applied to the closed-loop system. While on the contrary, $\lambda=0$ means that the reference cannot increase momentarily to ensure safety from constraints violation [21].

Remark 1: If $r(k)$ is an achievable output and remains constant since $t=k$, then $v(k)$ can converge to the reference $r(k)$ in finite time [36].

After incorporating the SRG design into the OFMPPC controller, the hierarchy of the proposed method can be shown in Fig. 2, where the position reference z_r is handled by SRG before being delivered to the well-designed offset-free MPC controller. And the detailed design procedure of the proposed method will be described in the following section.

B. Proposed OFMPPC-RG Method for PMSM

The OFMPPC-RG for PMSM position control is built based on the closed-loop system, where the OFMPPC controller in Section II serves as the main controller. The function of SRG is an add-on scheme for constraint handling and hardly influences the overall control performance. What is more, some specific modifications to SRG should be made to incorporate this technique into the PMSM control, and the detailed procedure is discussed as follows.

1) Coordinate Transformation: First, coordinate transformation should be made to convert (1) to (16) aiming for SRG design's convenience. Hence, the new state variables and the control can be defined as

$$
\begin{cases}
\bar{x}(k)=x(k)-x_{ss}\\
\bar{u}_q(k)=u_q(k)-u_{qss}\\
\bar{d}(k)=d(k)-\hat{d}(\infty)\approx 0
\end{cases}
\tag{19}
$$

where the steady state disturbance $\hat{d}(\infty)$ is assumed to be the same as $d(k)$. By plugging (19) into (1), the modified system can be expressed as (20) after simplification

$$
\bar{x}\left(k+1\right)=A\bar{x}(k)+B\bar{u}_q(k) \tag{20}
$$

with the updated constraint condition going as: $\bar{x}(k) \in [-x_{\max} - x_{ss}, x_{ax} - x_{ss}]$, $x_{ax} = (\infty, \omega_{\max}, I_{q\max})^T$, and $u(k) \in [-U_{q\max} - u_{qss}, U_{q\max} - u_{qss}]$.

By combining (19) with (11), the control signal after coordinate transformation takes the form of

$$\begin{aligned}\bar{u}_q(k) = & -K_{mpc1}\bar{x}(k) + K_{mpc3}U_{qss} - u_{qss} \\ & + K_{mpc2}\left(Z_r - Fx_{ss} - M\hat{d}(k)\right)\end{aligned} \tag{21}$$

where $K_{mpc1} = E_2(\Phi^T Q\Phi + W_R)^{-1}\Phi^T QF$
$K_{mpc2} = E_2(\Phi^T Q\Phi + W_R)^{-1}\Phi^T Q$
$K_{mpc3} = E_2(\Phi^T Q\Phi + W_R)^{-1}\Phi^T R.$

2) Closed-Loop System With SRG Formulation: Obviously, the overall closed-loop system can be acquired by combining (20) and (21) if the reference is replaced by the output signal $v(k)$ from the RG instead of the original position reference z_r

$$\begin{aligned}\bar{x}(k+1) = & (A - BK_{mpc1})\bar{x}(k) \\ & + B(-K_{mpc2}(Fx_{ss} \\ & + M\hat{d}(k)) + K_{mpc3}U_{qss} - u_{qss}) \\ & + Bv(k) = A_{cl}\bar{x}(k) + B(\xi(k)) + v(k)))\end{aligned} \tag{22}$$

where $v(k) = (1-\lambda)v(k-1) + \lambda r(k)$ is the output of SRG and the exact meaning of $r(k)$ is defined in the following section; $\xi(k)$ is the intermediate variable.

Remark 2: The position reference z_r can be smoothened to the trajectory $r(k)$ by (23) before the SRG algorithm takes effect to the benefit of a better performance and a stronger constraint handling ability in the PMSM position controller design. It is reasonable because the existence of a varying disturbance makes the maximal constraint admissible set O_∞ less achievable. Therefore, smoothing the position reference instead of a directly applied step reference is a compromise considering disturbances. Meanwhile, the rising rate of $r(k)$ is controlled by the smooth factor η, which also serves as an extra degree of freedom when tuning for a better response

$$r(k) = z_r e^{(-\eta(z_r - z(k)))}. \tag{23}$$

3) Maximal Constraint Admissible Condition: According to the SRG theory, the maximal constraint admissible condition (17) for the position control system (20) reduces to dealing with a series of inequalities as (24), that is, the system's states and control constraints for the future τ steps. Further, the state limitation can be expressed by (24a) as follows:

$$\begin{cases}\lambda R^\tau(r(k) - v(k-1)) \\ \quad \le x_{\max} - x_{ss} - A_{cl}^\tau\bar{x}(k) - R^\tau(\xi(k) + v(k-1)) \\ -\lambda R^\tau(r(k) - v(k-1)) \\ \quad \le x_{\max} + x_{ss} + A_{cl}^\tau\bar{x}(k) + R^\tau(\xi(k) + v(k-1))\end{cases} \tag{24a}$$

where $A_{cl}^\tau = (A_{cl})^\tau$ and $R^\tau = \sum_{i=0}^{\tau-1}(A_{cl})^i B$. Both matrices can be precomputed offline beforehand and stored in the memory, which will not add any extra calculation burden.

As for the control constraints on q-axis voltage, first the inequality set (24b) can be constructed to express the $t = k$th constraint on $u_q(k)$

$$\begin{cases}\lambda(r(k) - v(k-1)) \le U_{q\max} + K_{mpc1}x(k) \\ \quad + K_{mpc2}M\hat{d}(k) - K_{mpc3}U_{qss} - v(k-1) \\ -\lambda(r(k) - v(k-1)) \le U_{q\max} - K_{mpc1}x(k) \\ \quad - K_{mpc2}M\hat{d}(k) + K_{mpc3}U_{qss} + v(k-1).\end{cases} \tag{24b}$$

For the constraints on the subsequent control input from $u_q(k+1)$ to $u_q(k+\tau-1)$, (24c) forms the mathematical expression

$$\begin{cases}\lambda(1 - K_{mpc1}R^\tau)(r(k) - v(k-1)) \le U_{q\max} + K_{mpc1}R_d^\tau\hat{d}(k) \\ \quad - (1 - K_{mpc1}R^\tau)\left(K_{mpc3}U_{qss} - K_{mpc2}M\hat{d}(k)\right) \\ \quad + K_{mpc1}A_{cl}^\tau x(k) - (1 - K_{mpc1}R^\tau)v(k-1) \\ -\lambda(1 - K_{mpc1}R^\tau)(r(k) - v(k-1)) \le U_{q\max} - K_{mpc1}R_d^\tau\hat{d}(k) \\ \quad + (1 - K_{mpc1}R^\tau)\left(K_{mpc3}U_{qss} - K_{mpc2}M\hat{d}(k)\right) \\ \quad - K_{mpc1}A_{cl}^\tau x(k) + (1 - K_{mpc1}R^\tau)v(k-1)\end{cases} \tag{24c}$$

where matrix $R_d{}^\tau = \sum_{i=0}^{\tau-1}(A_{cl})^i B_d$.

Remark 3: Note that in all the inequalities previously, the q-axis current value in $x(k)$ should use the predicted value $\bar{i}_q(k+1)$ for the $t = k+1$ time instant to compensate for the time delay influence. And the prediction expression for $\bar{i}_q(k+1)$ can be written as

$$\begin{aligned}\bar{i}_q(k+1) = & \left(1 - \frac{TR}{L}\right)i_q(k) \\ & - \frac{p\psi_f T}{L}\omega(k) + \frac{T}{L}u_q(k-1) + \hat{d}_q(k).\end{aligned} \tag{25}$$

Remark 4: The range of the decision variable λ can be relaxed to $\lambda \in [\underline{\lambda}, \overline{\lambda}]$ for the proposed OFMPPC-RG method, which is based on the consideration of the disturbances in the PMSM system and the smoothened reference trajectory $r(k)$. By this design, $v(k)$ can be either smaller than $v(k-1)$ or more extensive than $r(k)$ in the SRG calculation.

Further, the problem (18) converts to solving the optimized λ^* within the range $\lambda \in [\underline{\lambda}, \overline{\lambda}]$ that satisfies the inequality set (24). In this work, the iteration number τ means that the SRG output $v(k)$ can guarantee constraint satisfaction in the future τ control periods. And the implementation steps of the proposed SRG algorithm on a well-designed offset-free MPC controller can be divided into two cases.

Case I: If the upper limits U_{qax} or x_{ax} are violated within the whole iterations, the proposed SRG degrades to the optimization problem (26) with only the upper bound inequalities considered, where a_{jk} and b_{jk} are the inequality coefficients calculated according to (24) within each control period. Typically, a_{jk} can be assumed to be positive for a fixed PMSM control system when the upper bound is hit

$$\begin{aligned}&\max\ \lambda \\ &\text{s.t.}\quad \begin{cases}\underline{\lambda} \le \lambda \le \overline{\lambda} \\ a_{jk}\lambda \le b_{jk}, j = 1,2,3; k = 1,\ldots,\tau.\end{cases}\end{aligned} \tag{26}$$

In fact, (26) can be solved quite efficiently by a fast solution method instead of calculating each solution of the inequalities for every iteration. The procedure, detailed in Algorithm 1,

Algorithm 1: Fast Solution Method of (26).

Input: Inequality coefficients a_{jk} and b_{jk}; bound $\underline{\lambda}$ and $\overline{\lambda}$; iteration number τ.

$\lambda_1 \leftarrow 1$; $k \leftarrow 1$; $j \leftarrow 1$;
while $k \leq \tau$ **do**
  while $j \leq 3$ **do**;
    if $a_{jk}\lambda_{jk} \geq b_{jk}$ **then** $\lambda_k = \min\{b_{jk}/a_{jk}, \lambda_k\}$;
    $j \leftarrow j + 1$;
  end while
  $\lambda_{k+1} \leftarrow \max\{\underline{\lambda}, \min\{\overline{\lambda}, \lambda_k\}\}$;
  $k \leftarrow k + 1$;
end while

Output: Optimal solution $\lambda^* = \lambda_{k+1}$ for (26).

begins by loading the coefficients a_{jk} and b_{jk} from memory and initializing the relevant variables (λ_1, k, and j) to 1. Within each iteration, the inequalities from (24a) to (24c) are sequentially evaluated until the maximum iteration number τ is reached. If any inequality is violated during the kth iteration, the value of λ_k is updated to its maximum admissible value to ensure that the constraint conditions remain satisfied. Upon completion of all iterations, the final value λ_{k+1} is clamped within the bounds $[\underline{\lambda}, \overline{\lambda}]$ and returned as the SRG output. The entire process involves only simple conditional checks and division operations, resulting in significantly reduced computational complexity.

Case II: When the system's states or the control input violate the lower bound ($-U_{qax}$ or $-x_{ax}$), the solution of SRG is equivalent to the optimization problem (27) corresponding to the lower bound inequalities. Typically, a_{jk} is negative in this case because the SRG output for PMSM tends to be bigger than the reference during decelerating. Following the same procedure as the fast solution algorithm previously, the maximum λ that satisfies (28) can be calculated efficiently

$$\max \lambda \quad \text{s.t.} \quad \begin{cases} \underline{\lambda} \leq \lambda \leq \overline{\lambda} \\ -a_{jk}\lambda \leq b_{jk}, j = 1, 2, 3; k = 1, \ldots, \tau. \end{cases} \tag{27}$$

Further, the implementation procedure of SRG can be summarized as follows. First, the inequality set (24) is checked by the states of PMSM $x(k)$ for $t = k$. If none of (24) is violated, λ is set to 1 and $r(k)$ can be directly given to the offset-free controller. If any of (24) is violated, the flow follows Cases I or II depending on whether the upper bound is hit or the lower bound is violated. Finally, the input trajectory $v(k)$ for $t = k$ is obtained with the resultant λ^* as (28). And offset-free position tracking will eventually be achieved when $v(k)$ converges to z_r

$$v(k) = (1 - \lambda^*)\, v\,(k-1) + \lambda^* r(k). \tag{28}$$

Before implementing the result in (28) to the well-designed OFMPPC controller, a low-pass filter (LPF) is built with a relatively high cutoff frequency ω_c as (29), where $v_{\text{final}}(s)$ is the final SRG output. The purpose is to filter out the high-frequency components caused by noise and varying disturbances. A smaller cutoff frequency ω_c results in stronger filtering but may degrade

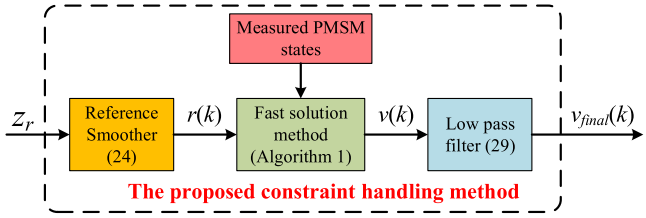

Fig. 3. Block diagram of the entire constraint handling flow.

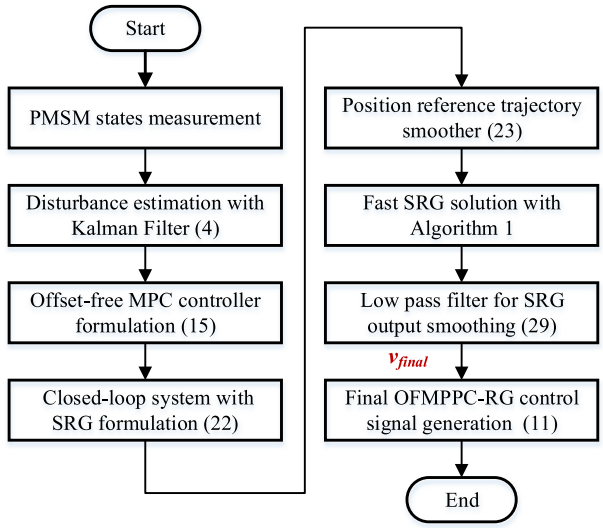

Fig. 4. Implementation flowchart of the proposed OFMPPC-RG method.

the system's dynamic response. Hence, it is advisable to select a relatively high ω_c value to strike a balance between effective chattering suppression and dynamic performance preservation

$$\frac{v_{\text{final}}(s)}{v(s)} = \frac{1}{s/\omega_c + 1}. \tag{29}$$

Obviously, the constraints can be well handled with only a series of inequality checks and arithmetic operations, which greatly reduces the calculation burden compared with iterative solvers. A brief block diagram of the entire constraint handling flow is displayed in Fig. 3 to provide a more straightforward view of our proposed method.

C. Implementation Steps and Parameter Tuning Methods

The implementation procedure and parameter tuning methodology of the proposed OFMPPC-RG approach are detailed in this section, with the corresponding flowchart presented in Fig. 4.

First, the operating states of the PMSM, including position and phase currents, are measured. Following state acquisition, disturbances in both the q-axis and speed loops are estimated using a Kalman filter-based disturbance observer, as described in (4), while the corresponding steady-state condition is determined from (6). Subsequently, constraints accounting for one step digital control delay are modeled, and the offset-free MPC

controller is formulated in (15), where the control signal is the solution of the constrained QP problem.

Once the controller is established, the constraint handling block is constructed. A coordinate transformation is applied to convert the closed-loop system's state equation into the SRG formulation. To mitigate the effects of varying disturbances, the reference trajectory is smoothed using (23) before solving the SRG problem with Algorithm 1. The SRG output $v(k)$, obtained from (28), is then processed through an LPF to attenuate high-frequency noise and suppress chattering in the control signal. The final output, denoted as v_{final}, is then used to replace the position reference in (11) and the resultant unconstrained MPC control signal $u_q(k)$ can be directly applied to the inverter.

In addition, the tuning strategy of key parameters is also illustrated as follows.

1) Prediction and Control Horizons N_p and N_c: The prediction horizon N_p should be large enough to cover the whole dynamics of the PMSM position response, preventing excessively reactive control decisions. A longer prediction horizon enhances stability and approximates the behavior of an optimal control (infinite horizon MPC case), thereby ensuring optimal performance during transient response. As for the control horizon N_c, empirical guidelines suggest setting it to approximately 1/3 or 1/5 of the prediction horizon, balancing computational complexity and system performance. However, $N_c \neq N_p$ will bring in truncation error which deteriorates the control performance. Since computational efficiency is not a limiting factor in the proposed method, a long enough N_p that covers the dynamics is preferred while $N_c = N_p$ is chosen to eliminate truncation errors entirely.

2) Weighting Factors q and w_R: From the cost function of our proposed offset-free MPC method (8), q and w_R penalizes the tracking error (performance priority) and the control (smoothness priority), respectively. Hence, a larger q means a more aggressive dynamics while a bigger w_R ensures a smoother control. Hence, the selection of q and w_R is a trial and error process in reality, guided by the desired system response characteristics specified by the control engineer.

3) Smooth Factor η and Iteration Number τ: The smooth factor η and iteration number τ determines the tightness of the feasible maximal constraint admissible set. A larger τ means a tighter maximal constraint admissible set so that the control signal turns to a less aggressive manner. As for the smooth factor, the smaller η is, the closer the smoothened trajectory to the step reference will be, which means a more aggressive response. In conclusion, the tuning of these two parameters depends on the disturbance level in the real applications and they are combined to determine the dynamical performance.

IV. Experimental Results

To verify the effectiveness of the proposed OFMPPC-RG method, experiments are conducted on a digital servo-PMSM system setup based on the PLECS/RTbox 2 platform, as shown in Fig. 5. This device is equipped with four 1.5 GHz ARM Cortex-A53 cores, 16 analog inputs and outputs, and 32 digital inputs and outputs, providing comprehensive interface support for encoders and current sensors. It serves as the controller with a PWM frequency of 5 kHz and can be controlled using a host PC connected via Ethernet. Meanwhile, a surface-mounted PMSM is used here with an external inertia pad, and the detailed electrical and mechanical parameters are listed in Table I. A dead-time of 0.8 us is introduced in the inverter, and the maximum allowable phase current and angular velocity are set to 3.6 A and 800 rpm, respectively. Both the prediction and control horizons are selected as 100, enabling long-horizon predictive control for accurate and robust position regulation.

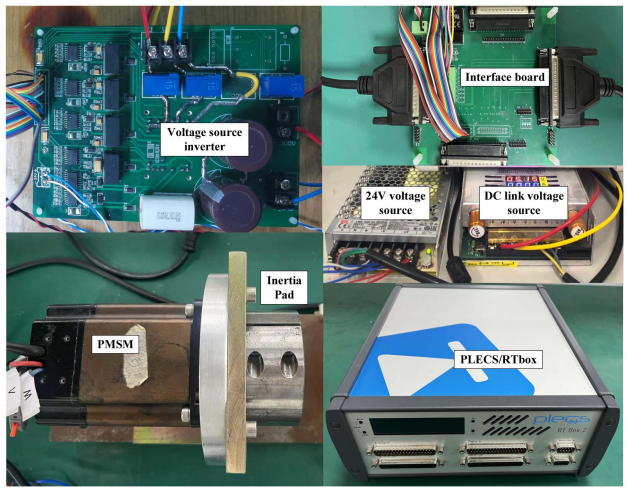

Fig. 5. Actual PMSM experimental platform.

TABLE I
Parameters Related to the Test Motor

Parameter	Value	Unit
Dc link voltage	62.5	V
Rated speed	1000	rpm
Pole pairs	5	
Flux linkage	0.059	Wb
Inertia	0.00129	kg·m^2
Inductan	0.003	H
Resistan	0.72	Ω

Experiments are carried out to demonstrate the whole operation scenario, including the step reference tracking test, the voltage constraint test, the effect of parameter change test, and robustness test. To evaluate the calculation time improvement compared with conventional iterative methods, two powerful solvers (Hildreth's algorithm from [34] and accelerated dual gradient projection (GPAD) algorithm from [17]) are used separately to solve the constrained QP problem in (15), and the methods are called OFMPPC-HA and OFMPPC-GPAD, respectively. Meanwhile, seven-step speed constraints and one-step current constraint are used to formulate the feasible region for the solver. What is more, the conventional three closed-loop position control structure is tested to show the proposed cascaded-free method's superiority. Since cascaded control performance can be largely improved by replacing traditional PI controllers by predictive controllers [5], both speed and current controllers

TABLE II
PERFORMANCE COMPARISON OF SETTLING TIME (2%) IN MILLISECONDS

Position reference (rad)	1	4	10
OFMPPC-RG (ms)	51.2	102.1	168.4
OFMPPC-GPAD (ms)	84.8	96.8	163.8
OFMPPC-HA (ms)	51.0	97.4	165.2
PCS (ms)	55.4	101.2	171.8

are updated by advanced predictive controllers (predictive functional control [37] and predictive current control [38], respectively) for the best control performance in the comparison. This combination provides strong evidence of the superiority of the proposed method. And the combined method is called predictive cascaded control in this brief. Meanwhile, all the parameters of the comparison methods are carefully tuned for the best control performance, and the experimental results are given as follows.

A. Step Tracking Test

Different position references (1, 4, and 10 rad) are given to the position controller to test the position step tracking performance of the proposed method, which covers the whole scenario of current limitation and speed constraint. Since the settling time (2% settling time) is a crucial index for evaluating the performance of a PMSM servosystem [39], the settling time of all the methods are listed in Table II, and the zoomed-in figures of transients are provided in the experimental results. The parameter pair of the OFMPPC-RG (q, w_R, η, τ) is tuned as (840, 0.5, 0.27, 20) for the 1 rad case, (200, 0.5, 0.055, 38) for the 4 rad case, and (200, 0.5, 0.04, 25) for the 10 rad case, respectively.

Fig. 6–9 show the experimental results when the position reference changes from 1 to 10 rad, where a step reference is set. Two key indices, 2% error band settling time and average static position errors (ASPEs) within 0.1 s, are calculated to evaluate the position control performance [14]. And the ASPE is defined as (30). In the results for all the three cascaded-free methods, the filtered position reference from SRG (denoted by v in the figures), position feedback θ, dq-axis current, dq-axis voltage, and the observed disturbances are given. For the predictive cascaded control method, the motor speed result is provided because no observer is included here. For the 1 rad position reference case shown in Fig. 6, the weighting factor q is deliberately tuned to a larger value than in typical operating conditions to induce a more aggressive q-axis current response, thereby highlighting the effectiveness of the proposed constraint-handling strategy. Hence, the position response profile oscillates in transients for the offset-free based controllers, but their amplitudes are acceptable within the 2% error band

$$\text{ASPE} = \frac{1}{N}\sum_{i=1}^{N}|\theta(i) - z_r|. \tag{30}$$

From the results, all of the four methods can effectively limit the system's constraints (current, voltage, and speed). However, the proposed OFMPPC-RG method exhibits a much smaller overshoot as well as the oscillation in the q-axis current control performance than the other three methods, which is

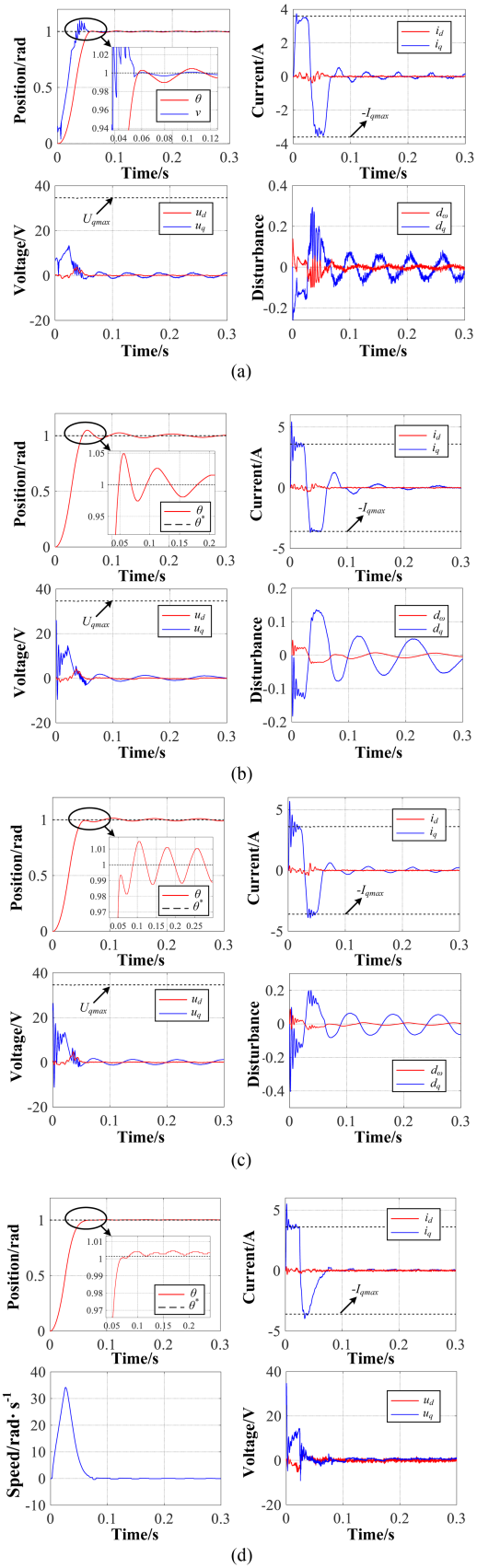

Fig. 6. Performance comparison under different control strategies with 1 rad reference position. (a) Proposed OFMPPC-RG method. (b) OFMPPC-GPAD method. (c) OFMPPC-HA method. (d) Predictive cascaded control method.

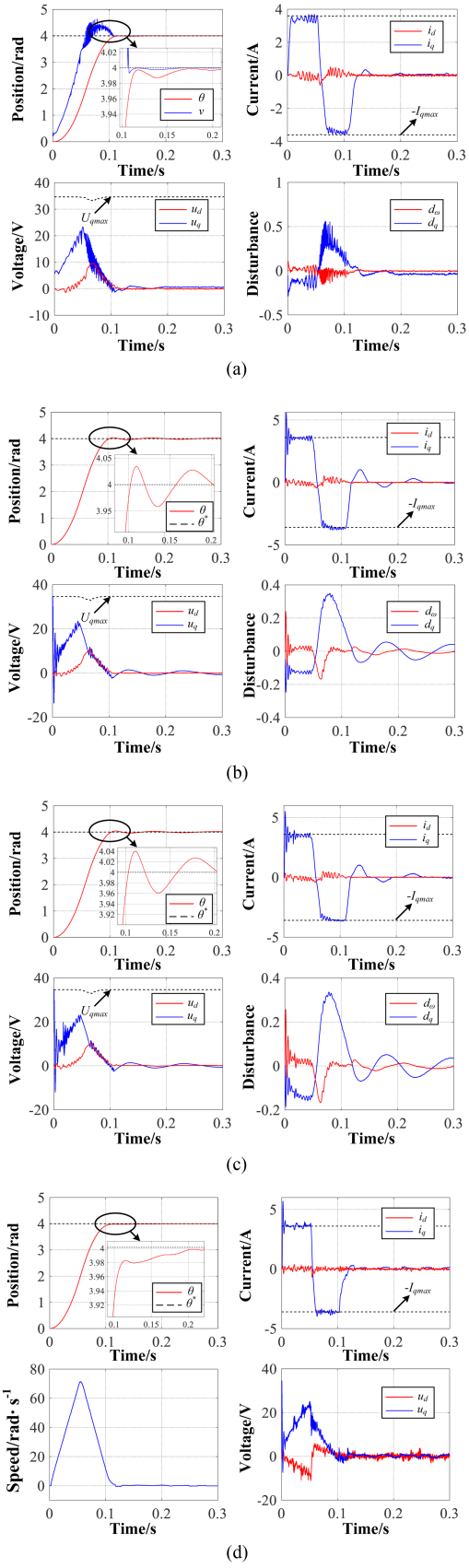

Fig. 7. Performance comparison under different control strategies with 4 rad reference position. (a) Proposed OFMPPC-RG method. (b) OFMPPC-GPAD method. (c) OFMPPC-HA method. (d) Predictive cascaded control method.

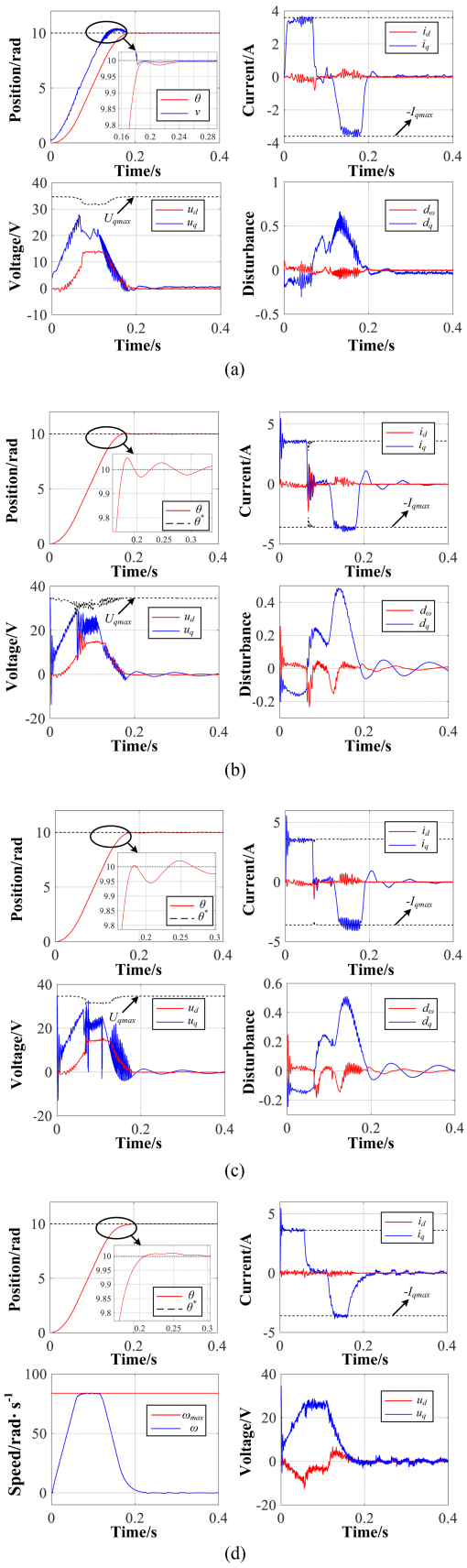

Fig. 8. Performance comparison under different control strategies with 10 rad reference position. (a) Proposed OFMPPC-RG method. (b) OFMPPC-GPAD method. (c) OFMPPC-HA method. (d) Predictive cascaded control method.

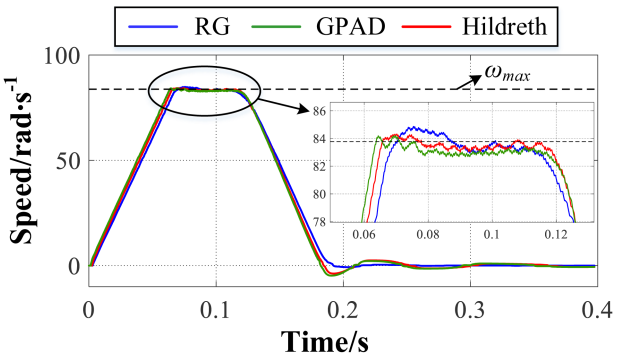

Fig. 9. Speed constraints handling performance comparison under different constraint handling strategies (OFMPPC-RG, OFMPPC-GPAD, and OFMPPC-HA) under 10 rad reference position.

TABLE III
PERFORMANCE COMPARISON OF ASPE IN ANGLE

Position reference (rad)	1	4	10
OFMPPC-RG (rad)	0.0025	0.00082	0.00079
OFMPPC-GPAD (rad)	0.0087	0.0139	0.0094
OFMPPC-HA (rad)	0.0069	0.0132	0.0101
PCS (rad)	0.0018	0.0016	0.0011

TABLE IV
CALCULATION TIME COMPARISON IN MICROSECONDS

Position reference (rad)	1	4	10
OFMPPC-RG (μs)	5.78	6.87	5.86
OFMPPC-GPAD (μs)	7.69	14.51	166.47
OFMPPC-HA (μs)	16.07	15.32	120.59

more favorable for the motor drive's safety operation. Also, the performance comparison of settling time is shown in Table II for all the four methods. Obviously, the three offset-free MPC-based position control methods tend to hold faster response speed than the predictive cascaded control structure, which attributes to the bandwidth improvement of the cascaded-free structure. The settling time of solver-based solutions is shorter than the proposed OFMPPC-RG method, which is reasonable because the proposed SRG constraint handling strategy acts as a filter and the calculation burden reduction is realized at the cost of a slower response speed. Even so, the response speed is still faster compared with the most advanced predictive cascaded control structure in the 1 and 10 rad cases, not to mention the performance improvement over the conventional three closed-loop PI method.

Meanwhile, the ASPE index comparison of the four methods is given in Table III, which is an important index evaluating the steady state tracking precision. It can be concluded that the proposed method has the best steady state performance (0.0025 for 1 rad, 0.00082 for 4 rad, and 0.00079 for 10 rad) while much better than other solver-based offset-free MPC controllers.

As for the computational burden reduction of the proposed method, Table IV shows the calculation time of all the cascaded-free MPC methods. Note that the predictive cascaded control method is not included in the comparison because cascaded methods can limit states by merely incorporating a saturation block at the end of each loop's output. In addition, there is no meaningful comparison in terms of calculation time with methods that involve solving a constrained QP problem. From the results, it can be concluded that the proposed OFMPPC-RG method significantly reduces the calculation burden for all three reference cases compared to solver-based optimization methods. The reduction becomes more pronounced when the speed constraint is activated in the 10 rad position reference scenario. In this case, both the OFMPPC-HA and OFMPPC-GPAD methods fail to converge to the desired resolution within the prescribed iteration limit, as the inclusion of seven additional speed constraint steps substantially increases both the number of iterations required and the computational burden per iteration. In comparison, the proposed method can successfully handle speed, current, and voltage constraints simultaneously with hardly any increase in calculation burden as seen in the 1 and 4 rad cases. Besides, Fig. 9 shows the motor speed result under the 10 rad case with three offset-free predictive control strategies. Obviously, all the motor speed can be restricted within the limitation value effectively. And the speed curve exhibits a smoother profile with the proposed OFMPPC-RG method when the motor position reaches the reference's neighborhood, which means less oscillation in the position control performance.

B. Voltage Constraint Verification

In the previous section, the voltage constraint ability is not sufficiently verified, as the relatively high dc-link voltage makes it difficult for the control voltage to reach the limit in the current transient. To demonstrate the effectiveness of the voltage constraint handling with the proposed OFMPPC-RG method, an additional test scenario is deliberately designed to induce an overvoltage condition, where the dc-link voltage U_{dc} is set as 20 V with 1 rad position reference. As shown in Fig. 10(b), the proposed OFMPPC-RG successfully constrains the q-axis voltage throughout the entire operation. Meanwhile, the dq-axis currents and motor speed remain well-regulated under this condition, as illustrated in Fig. 10(c) and (d).

C. Effect of Parameter Change in the Proposed Controller

This set of experiments is designed to elucidate the influence of two key tuning parameters in the proposed method, namely the smoothing factor η and the iteration number τ, on the system's control performance. The tuning principles for both parameters have been discussed previously. Fig. 11 illustrates the effect of varying η with the same 1 rad position reference. As employed in (23), η introduces no additional computational burden. The results indicate that η serves to smooth the position reference trajectory, where a smaller value yields a more aggressive control response.

Regarding the iteration number τ, increasing its value results in a more conservative constraint admissible set. Since the SRG output is primarily determined by the scalar λ, higher τ values tend to yield more conservative behaviors and extended transient durations. As defined in Algorithm 1, τ dictates the number of times the inequality set (24) is evaluated (steps 2–9), implying that greater τ leads to longer computation time. Fig. 12 presents

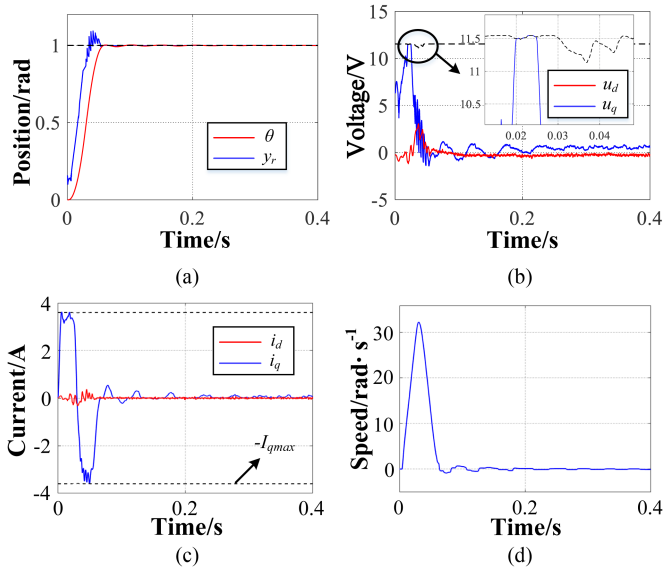

Fig. 10. Voltage constraints handling verification of the proposed OFMPPC-RG method under 1 rad reference position when U_{dc} is set as 20V. (a) SRG output and motor position. (b) dq-axis voltage and limitation. (c) dq-axis current and limitation. (d) Motor speed.

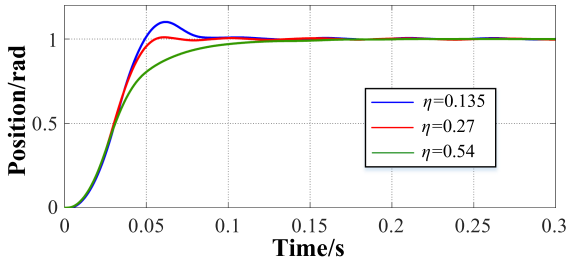

Fig. 11. Effect of the smooth factor η on the position control performance of the proposed OFMPPC-RG method under 1 rad reference position.

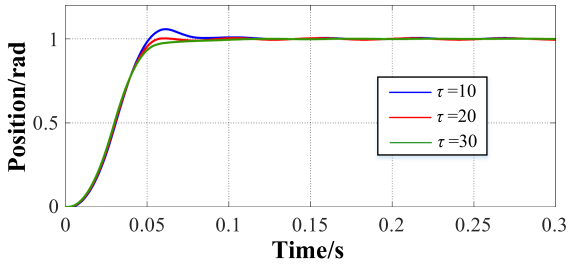

Fig. 12. Effect of the iteration number τ on the position control performance of the proposed OFMPPC-RG method under 1 rad reference position.

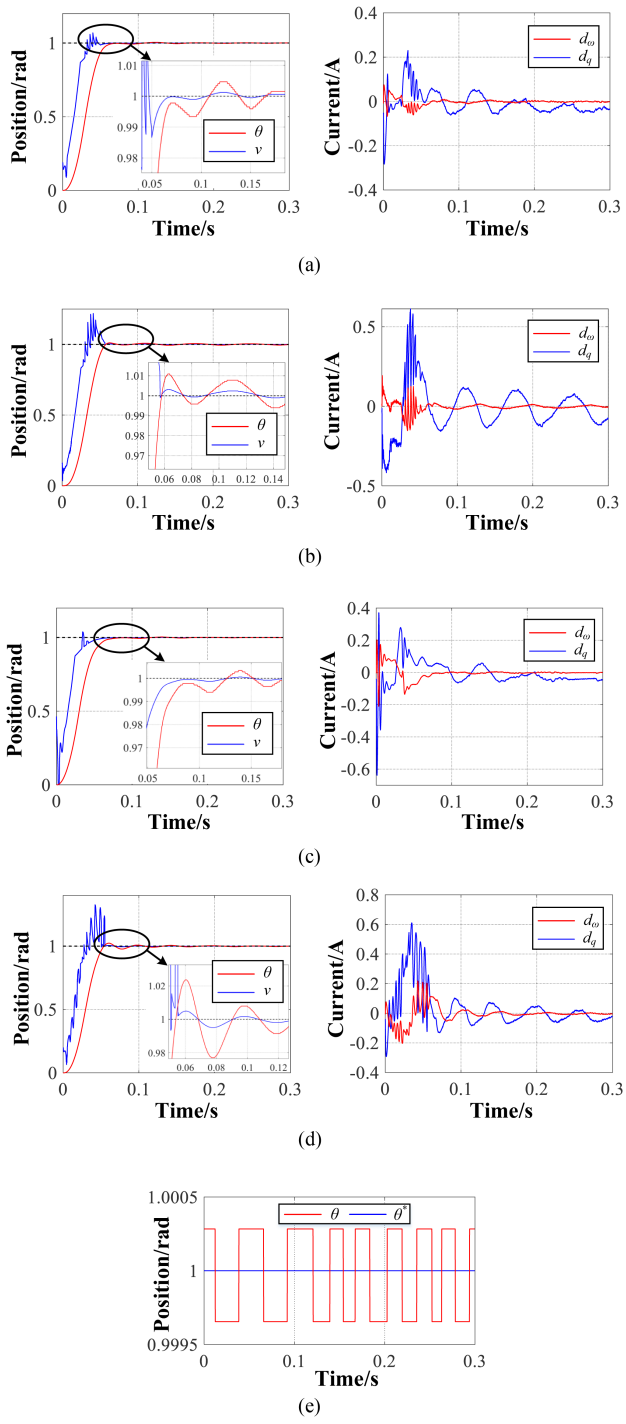

Fig. 13. Position tracking performance of the proposed OFMPPC-RG method on 1 rad under different parameter mismatches. (a) 50% resistance mismatch. (b) 50% inductance mismatch. (c) 50% inertia mismatch. (d) 50% flux linkage mismatch. (e) Zoomed-in steady state performance under 50% inertia mismatch.

a comparative analysis under different τ values, confirming this relationship. However, excessive τ may result in the infeasibility of the optimization problem in (18) and should thus be avoided.

As a result, τ and η significantly impact the system's position control performance and must be tuned carefully through trial and error to achieve an optimal balance between dynamic response and constraint satisfaction.

D. Robustness Test

One significant advantage of the proposed OFMPPC-RG method lies in its enhanced robustness, achieved through offset-free tracking enabled by the integration of a disturbance observer (Kalman filter). According to the state–space model in (1), the tracking performance of the proposed method may be influenced

by variations in key motor parameters, including rotor inertia J, stator inductance L, flux linkage ψ_f, and stator resistance R. To evaluate this sensitivity, robustness tests are conducted under 50% mismatch on each parameter, with the corresponding results presented in Fig. 13.

Despite these substantial mismatches, the system maintains stable operation. The settling times under resistance, inductance, inertia, and flux linkage mismatches are 57.2, 54.8, 63.8, and 62.8 ms, respectively, indicating only slight degradation in transient performance. This increase in settling time is primarily attributed to the shift in system eigenvalues caused by discrepancies between nominal and actual parameters. Nevertheless, due to the offset-free control structure, the system continues to achieve zero steady-state error even under these mismatched conditions. This validates the disturbance estimation capability of the Kalman filter in handling lumped uncertainties. For illustration, the zoomed-in steady-state performance under 50% inertia mismatch is provided in Fig. 13(d), further confirming the effectiveness of the proposed approach.

V. Conclusion

This article proposes a novel OFMPPC-RG method for the SPMSM position servoapplications. The proposed approach adopts a cascade-free control architecture to enhance system dynamics. An offset-free MPC scheme is developed to improve both control accuracy and disturbance rejection capabilities. Moreover, a computationally efficient constraint-handling strategy based on SRG theory is introduced, which significantly reduces the computational burden compared to conventional solver-based approaches. Experimental results validate the proposed method's effectiveness in achieving fast dynamic response, strong robustness, effective constraint handling, and reduced computational complexity, thereby improving the practical applicability of MPC in real-time position control scenarios.

Appendix

Proof of (2)'s observability: The augmented PMSM system (2) is observable if and only if the pair (C, A) is observable and the following matrix (31) has full column rank:

$$\begin{bmatrix} A-\mathbf{I} & B_d \\ C & 0 \end{bmatrix}. \tag{31}$$

Proof: This article gives a simple proof of this theorem according to the procedure in [40]. Obviously, the pair (C, A) is observable for a given PMSM system. According to Popov–Belevitch–Hautus (PBH) criterion, the following expression holds:

$$\text{Rank}\left(\begin{bmatrix} A^T-\lambda\mathbf{I} & C^T \end{bmatrix}\right) = n.$$

If we apply the PBH criterion to the augmented system matrix, (2) is observable if and only if the matrix

$$\begin{bmatrix} A^T-\lambda\mathbf{I} & 0 & C^T \\ B_d^T & \mathbf{I}-\lambda\mathbf{I} & 0 \end{bmatrix}$$

has full row rank, which is obvious for $\lambda \neq 1$. Hence, only the $\lambda = 1$ case should be checked for the PBH condition to hold, where the augmented system matrix degrades to (31). ■

References

[1] Y. Xu, S. Jin, S. Li, X. Zhang, and J. Zou, "A novel finite position set phase-locked loop strategy for PMSM position estimation with high-precision and low computational burden," *IEEE Trans. Power Electron.*, vol. 40, no. 1, pp. 1622–1635, Jan. 2025.

[2] X. Sun, J. Cao, G. Lei, Y. Guo, and J. Zhu, "A robust deadbeat predictive controller with delay compensation based on composite sliding-mode observer for PMSMs," *IEEE Trans. Power Electron.*, vol. 36, no. 9, pp. 10742–10752, Sep. 2021.

[3] W. Sun, J. Liu, and H. Gao, "A composite high-speed and high-precision positioning approach for dual-drive gantry stage," *IEEE Trans. Automat. Sci. Eng.*, vol. 22, pp. 2514–2525, 2025.

[4] B. Tang, W. Lu, B. Yan, K. Lu, J. Feng, and L. Guo, "A novel position speed integrated sliding mode variable structure controller for position control of PMSM," *IEEE Trans. Ind. Electron.*, vol. 69, no. 12, pp. 12621–12631, Dec. 2022.

[5] C. Garcia, J. Rodriguez, C. Silva, C. Rojas, P. Zanchetta, and H. Abu-Rub, "Full predictive cascaded speed and current control of an induction machine," *IEEE Trans. Energy Convers.*, vol. 31, no. 3, pp. 1059–1067, Sep. 2016.

[6] Z. Zhang, X. Liu, J. Yu, and H. Yu, "Time-varying disturbance observer based improved sliding mode single-loop control of PMSM drives with a hybrid reaching law," *IEEE Trans. Energy Convers.*, vol. 38, no. 4, pp. 2539–2549, Dec. 2023.

[7] G. Yu et al., "Full-speed region control method based on deadbeat direct speed control for SPMSMs," *IEEE Trans. Emerg. Sel. Topics Power Electron.*, vol. 12, no. 5, pp. 4900–4915, Oct. 2024.

[8] J. Rodriguez et al., "Latest advances of model predictive control in electrical drives–Part I: Basic concepts and advanced strategies," *IEEE Trans. Power Electron.*, vol. 37, no. 4, pp. 3927–3942, Apr. 2022.

[9] X. Gao, M. Abdelrahem, C. M. Hackl, Z. Zhang, and R. Kennel, "Direct predictive speed control with a sliding manifold term for PMSM drives," *IEEE Trans. Emerg. Sel. Topics Power Electron.*, vol. 8, no. 2, pp. 1258–1267, Jun. 2020.

[10] J. Hu, C. He, and Y. Li, "A novel predictive position control with current and speed limits for PMSM drives based on weighting factors elimination," *IEEE Trans. Ind. Electron.*, vol. 69, no. 12, pp. 12458–12468, Dec. 2022.

[11] F. Niu et al., "Cooperative predictive position control of dual-motor system," *IEEE Trans. Emerg. Sel. Topics Power Electron.*, vol. 10, no. 6, pp. 7560–7568, Dec. 2022.

[12] G. Cimini, D. Bernardini, S. Levijoki, and A. Bemporad, "Embedded model predictive control with certified real-time optimization for synchronous motors," *IEEE Trans. Control Syst. Technol.*, vol. 29, no. 2, pp. 893–900, Mar. 2021.

[13] C. He, J. Hu, X. Ran, F. Wei, Y. Li, and Y. Zhu, "A simplified constrained predictive position control for PMSM drives with laguerre functions," *IEEE Trans. Ind. Electron.*, vol. 71, no. 12, pp. 15478–15487, Dec. 2024.

[14] C. He, J. Hu, and Y. Li, "Predictive position control with system constraints for PMSM drives based on geometric optimization," *IEEE Trans. Ind. Electron.*, vol. 70, no. 8, pp. 7773–7782, Aug. 2023.

[15] K. Belda and D. Vosmik, "Explicit generalized predictive control of speed and position of PMSM drives," *IEEE Trans. Ind. Electron.*, vol. 63, no. 6, pp. 3889–3896, Jun. 2016.

[16] D. Arnstrom, A. Bemporad, and D. Axehill, "A dual active-set solver for embedded quadratic programming using recursive LDL^T updates," *IEEE Trans. Autom. Control*, vol. 67, no. 8, pp. 4362–4369, Aug. 2022.

[17] P. Patrinos and A. Bemporad, "An accelerated dual gradient-projection algorithm for embedded linear model predictive control," *IEEE Trans. Autom. Control*, vol. 59, no. 1, pp. 18–33, Jan. 2014.

[18] S.-X. Wen, Z.-R. Pan, K.-Z. Liu, X. Zhang, and X.-M. Sun, "Practical offset-free model predictive control and its embedded application to aero-engines," *IEEE Trans. Automat. Sci. Eng.*, vol. 21, no. 4, pp. 7016–7026, Oct. 2024.

[19] X. Liu et al., "Continuous control set predictive speed control of SPMSM drives with short prediction horizon," *IEEE Trans. Power Electron.*, vol. 37, no. 9, pp. 10166–10177, Sep. 2022.

[20] X. Jiang et al., "An improved implicit model predictive current control with continuous control set for PMSM drives," *IEEE Trans. Transport. Electrific.*, vol. 8, no. 2, pp. 2444–2455, Jun. 2022.

[21] E. Garone, S. Di Cairano, and I. Kolmanovsky, "Reference and command governors for systems with constraints: A survey on theory and applications," *Automatica*, vol. 75, no. 1, pp. 306–328, 2017.
[22] S. Di Cairano, A. Goldsmith, U. V. Kalabic, and S. A. Bortoff, "Cascaded reference governor-MPC for motion control of two-stage manufacturing machines," *IEEE Trans. Control Syst. Technol.*, vol. 27, no. 5, pp. 2030–2044, Sep. 2019.
[23] I. Kolmanovsky, E. Garone, and S. Di Cairano, "Reference and command governors: A tutorial on their theory and automotive applications," in *Proc. Amer. Control Conf.*, 2014, pp. 226–241.
[24] M. M. Nicotra, D. Liao-McPherson, and I. V. Kolmanovsky, "Embedding constrained model predictive control in a continuous-time dynamic feedback," *IEEE Trans. Autom. Control*, vol. 64, no. 5, pp. 1932–1946, May 2019.
[25] C. S. Lim, S. S. Lee, and E. Levi, "Continuous-control-set model predictive current control of asymmetrical six-phase drives considering system nonidealities," *IEEE Trans. Ind. Electron.*, vol. 70, no. 8, pp. 7615–7626, Aug. 2023.
[26] Y. Xu, S. Li, and J. Zou, "Integral sliding mode control based deadbeat predictive current control for PMSM drives with disturbance rejection," *IEEE Trans. Power Electron.*, vol. 37, no. 3, pp. 2845–2856, Mar. 2022.
[27] J. Yang, W.-H. Chen, S. Li, L. Guo, and Y. Yan, "Disturbance/uncertainty estimation and attenuation techniques in PMSM drives-A survey," *IEEE Trans. Ind. Electron.*, vol. 64, no. 4, pp. 3273–3285, Apr. 2017.
[28] Z. Zhang, Y. Liu, X. Liang, H. Guo, and X. Zhuang, "Robust model predictive current control of PMSM based on nonlinear extended state observer," *IEEE Trans. Emerg. Sel. Topics Power Electron.*, vol. 11, no. 1, pp. 862–873, Feb. 2023.
[29] K. Zuo, F. Wang, K. Luo, L. He, R. Kennel, and M. L. Heldwein, "Model optimization strategy based on moving horizon estimation for induction motor," *IEEE Trans. Energy Convers.*, vol. 39, no. 2, pp. 884–895, Jun. 2024.
[30] T. Guo, Z. Sun, X. Wang, S. Li, and K. Zhang, "A simple current-constrained controller for permanent-magnet synchronous motor," *IEEE Trans. Ind. Informat.*, vol. 15, no. 3, pp. 1486–1495, Mar. 2019.
[31] C. Dai, T. Guo, J. Yang, and S. Li, "A disturbance observer-based current-constrained controller for speed regulation of PMSM systems subject to unmatched disturbances," *IEEE Trans. Ind. Electron.*, vol. 68, no. 1, pp. 767–775, Jan. 2021.
[32] Y. Xu, S. Li, W. Zhang, G. Yu, and J. Zou, "Long-horizon constrained model predictive direct speed control for PMSM drives based on Laguerre functions," *IEEE Trans. Control Syst. Technol.*, vol. 32, no. 3, pp. 1002–1014, May 2024.
[33] B. Amini and R. R. Bitmead, "LQG control performance with low-bitrate periodic coding," *IEEE Trans. Control Netw. Syst.*, vol. 9, no. 1, pp. 320–333, Mar. 2022.
[34] L. Wang, *Model Predictive Control System Design and Implementation Using MATLAB*. London, U.K.: Springer-Verlag, 2009.
[35] S. Boyd and L. Vandenberghe, *Convex Optimization*. Cambridge, U.K.: Cambridge Univ. Press, 2004.
[36] E. Gilbert and I. Kolmanovsky, "Fast reference governors for systems with state and control constraints and disturbance inputs," *Int. J. Robust Nonlinear Control*, vol. 9, no. 15, pp. 1117–1141, 1999.
[37] H. Liu and S. Li, "Speed control for PMSM servo system using predictive functional control and extended state observer," *IEEE Trans. Ind. Electron.*, vol. 59, no. 2, pp. 1171–1183, Feb. 2012.
[38] T. Turker, U. Buyukkeles, and A. F. Bakan, "A robust predictive current controller for PMSM drives," *IEEE Trans. Ind. Electron.*, vol. 63, no. 6, pp. 3906–3914, Jun. 2016.
[39] S. Li, Y. Xu, W. Zhang, and J. Zou, "A novel two-phase mode switching control strategy for PMSM position servo systems with fast-response and high-precision," *IEEE Trans. Power Electron.*, vol. 38, no. 1, pp. 803–815, Jan. 2023.
[40] F. Borrelli, A. Bemporad, and M. Morari, *Predictive Control for Linear and Hybrid Systems*. Cambridge, U.K.: Cambridge Univ. Press, 2017.